JNPS 10 (2): 121 – 127 (2024)
ISSN: 2392-473X (Print), 2738-9537 (Online)

Research Article ©*Nepal Physical Society*
doi.org/10.3126/jnphyssoc.v10i2.79499

Adsorption of Molecular Methane on Strained Silicene

Suraj Rai,[1] Rajendra Prasad Adhikari,[2] and Nurapati Pantha[1, *)]

[1)]*Central Department of Physics, Tribhuvan University, Kirtipur*
[2)]*Department of Physics, Kathmandu University, Dhulikhel*

Abstract. Silicene has drawn enormous research interest due to its extraordinary properties and potential applications. We performed first-principles calculations to study the geometrical, electronic and stability related properties of silicene under uniaxial strain. Our results show a finite band gap in strained silicene instead of zero gap Dirac cone in pristine one. Furthermore, the adsorption energy of methane is found to be higher in strained silicene compared to unstrained silicene, relevant for storing energy-carrying gases at operating conditions.

Submitted:October 16, 2024; **Revised**: May 30, 2025; **Accepted**: June 1, 2025

Keywords: Silicene; Adsorption Energy; Uniaxial Strain; Methane; Energy-Carrying Gases

1. INTRODUCTION

After the isolation of graphene as a monolayer of carbon atoms from the bulk graphite in 2004 [1], two dimensional (2D) materials have drawn worldwide attention. This stimulated interesting questions to investigate new 2D and nano materials with unique and exotic properties [2].

Despite the pioneer surface structure and promising properties of graphene, it is difficult to integrate carbon materials with current silicon-based industry. Several other 2D materials (for example, hexagonal boron nitride (h-BN), and molybdenum disulfide (MoS_2)) exhibit a rich spectrum of properties and have been explored to incorporate layered-structures into devices. Furthermore it is important to obtain a single crystal of large size for characterization and device fabrication, especially for efficient low-budget mechanical/electronic devices. Researchers proposed a two-dimensional allotrope of silicon, Silicene, as a substitute for graphene [3]. However, unlike planar graphene, silicene forms a buckled hexagonal shape because electrons of Si- atom tend to form sp^3 hybridization rather than sp^2 hybridization [4]. Its buckled structure permits not only a tunable bandgap in the presence of an external electric field [5] but also highly chemically active on the surface and allows chemical functionalization to tune its electronic states.

*)Corresponding author: mrnurapati@gmail.com

Besides, silicene exhibits several notable advantages over graphene: a much stronger spin-orbit coupling, which may lead to a realization of the quantum spin Hall effect in the experimentally accessible temperature; a better tunability of the bandgap, which is essential for a productive field-effect transistor (FET) operating at room temperature; an easier valley polarization and more suitability for valleytronics study [4]. These make Silicene more desirable for the development of nanoelectronics and superior to easily being incorporated into silicon-based electronic technology. Because silicene has these surprising properties that the other 2D materials do not manifest, the functionalization of silicene by adsorption of molecules is expected to be different from the other well-known 2D materials [6].

Takeda and Shiraishi, in 1994, investigated the atomic and electronic structure of silicene for the first time [7]. In 2005, silicene began to appear in various theoretical and experimental studies. Le Lay synthesized self-aligned one-dimensional (1D) structures of silicon on Ag(110) surface [8]. The name 'Silicene' was coined in 2007 for the first time when the planar structure of silicene was investigated using tight-binding Hamiltonians. Further, it was underlined that similar to graphene, the planar structure of silicene would also reflect linearly crossing bands at the Fermi level [9].

Although the synthesis of free-standing Silicene is daunting task, it was experimentally fabricated on different substrates like $Ar(111)$, MoS_2, and ZrB_2 (001) [8], [10], [11]. The first compelling experimental evidence for the existence of silicene was reported in 2012. They deposited silicon on top of an $Ag(111)$ substrate instead of $Ag(110)$. Although not directly imaged, a monolayer

of silicene with 3×3 reconstruction was observed, which was perfectly in agreement with the 4×4 supercell of the Ag(111) surface [12].

1.1. Strain

Previous studies have demonstrated that strain engineering can be a promising way of tuning the electronic properties of either bulk Si or one-dimensional Si nanowires and it is also considered to be one of the best strategies for developing high-performance sub-10-nm silicon devices [13]. For instance, strain can enhance electron mobility and reduce the effective mass of the carriers of bulk Si, and Si-nanowires [14]. Topskal et. al also reported that the lattice strain is a useful method for modulating band structure in designing electronics devices and for developing high-performance [15]. The strain effects on the band structure are pivotal to understanding because they can boost the growth of silicene on a substrate with different lattice constants. Furthermore, strain enables the tunability of bandgap in a semiconductor, which is promising for the application of silicene in nanoelectronics or current silicon-based technology [16]- [17]. Like graphene, silicene is a zero bandgap semimetal. A glut of methods has been proposed to induce a bandgap in silicene sheet including doping, substrate effects, chemical functionalization, electric field, nanomesh, and nanoholes. Strain application is one of the possible methods to induce a bandgap. Qin et al. (2012) [17] observed that the semimetal state of silicene changes into a conventional metal for larger strains; the biaxial strain significantly changed the work function. Wella et al. (2015) found that applying the strain to the silicene gives a positive response to make silicene a candidate for sensing gas, especially to detect molecular H_2S [18]. Wu et al. demonstrated that biaxial strain and uniaxial tensile strain along the armchair direction can lessen the energy barrier of dissociative H_2 adsorption on silicene significantly, and the barrier reduces as the strain's rise. On the ground of this reality, a comprehensive study on the strain effect is promising.

The strain is defined by

$$\varepsilon = \frac{a - a_0}{a_0} \tag{1}$$

where a and a_0 represent the strained and initial lattice parameters respectively.

Last decade has witnessed a dramatic advancement in the application of 2D materials in nano/microelectronic devices such as high-performance field-effect transistors, transparent conductive films, and ultrathin solar cells. This growth is primarily based on an improved comprehension and advanced modulation of these materials, including graphene, MoS_2, and Bi_2Te_3, etc. To accomplish the goal of modulating the electronic/magnetic properties of 2D materials, and the adsorption behavior of molecules on their surface or edge sites different modifications have been broadly applied. The method of modification can be application of strain, vacancy, doping or functionalization of 2D materials which are expected to meet industrial demands [6]. Previous works in the similar field have addressed the impact of vacancy on gasesous adsorption, however, the effect of strain on silicene for its reactivity towards small gas molecules like CH_4 is still unsetteled question [19]. Methane, the primary constituent of natural gas, has been broadly used as fuel and source for producing other utilitarian chemicals. Moreover, methane is one of the prominent pollutant gases and can be useful on proper handling [20], [21]. In the present study, we aim to analyze the effect of increasing strain on silicene so that it can be useful as sensor and/or storing device changing nature of interaction between the constituents via density functional theory based calculations.

2. COMPUTATIONAL METHODS

We have performed the density functional theory based first-principles calculations to investigate the structural stability, electronic properties and magnetic properties of both pristine and strained silicene incorporating van der Waals (vdW) interactions in Quantum ESPRESSO codes [22, 23, 24]. The generalized gradient approximation (GGA) developed by three scientists Perdew, Burke and Ernzerhof (PBE) [25] was used to incorporate the electronic exchange and correlation effect. Similarly, Kresse-Joubert(KJ) projector augmented wave(PAW) pseudopotential was used to replace the complex effects of electrons and its nucleus. During the calculations, structure was allowed to relax under Broyden-Fletcher-Goldfarb-Shanno (BFGS) [26] scheme until the total energy change was less than 10^{-4} Ry between two consecutive self-consistent fields (scf) steps and each component of force acting was less than 10^{-3} Ry/Bohrs to get geometrically optimized structure. The method of convergence test was used to fix charge density cutoff. The 'Marzarri-Vanderbilt (m-v)' [27] smearing with mixing factor of 0.3 was used for self-consistency. Grimme model of van der Waals correction was employed for long range interactions. The total energy in this case is

$$E_{tot} = E_{DFT} + E_{disp} \tag{2}$$

where E_{tot} is the total energy, E_{DFT} is energy with a given exchange-correlation functional and E_{disp} is the dispersive interaction contribution.

For the binding behavior of methane gas molecule on both pristine and strained Silicene, we calculated the adsorption energy E_{ad}. This value addresses the binding

mechanism and structural stability of the molecule. It is calculated by:

$$E_{ad} = E_{Si+molecule} - E_{Si} - E_{molecule} \quad (3)$$

where, $E_{Si+molecule}$, E_{Si}, and $E_{molecule}$ denote the energy of silicene-methane system, pristine Silicene, and isolated gas molecule (CH_4 in our case) respectively.

We've also performed Bader charge analysis to study the nature of interaction and to calculate the exchange of electronic charge between guest and host materials.

3. RESULTS AND DISCUSSION

3.1. Geometry and Formation energy

Supercell (4×4) of pure silicene monolayer contains 32 atoms Figure 1 and was constructed by using the coordinates and lattice parameters from references [28]. The structure was then optimized and found the lattice parameters (a = b = 15.48 Å). The interlayer separation (c) was set 19.65 Åto avoid possible interaction between the layers.

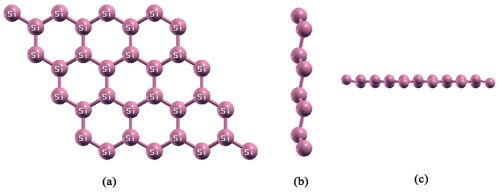

FIGURE 1: (a) Top View, (b) Side View (Xz Plane) And (c) Side View (In Yz Plane) Of 4×4 Supercell Of Monolayer Silicene

The monolayer silicene has honeycomb type of bravais lattice with buckled atomic arrangement Figure 1. The strain along the longitudnal x-direction was set to 1%, 3%, 5%, 7% and 8% respectively to study its effect on structural, electronic and magnetic properties.mThis range of strain engineering has been selected to check the material properties in wider level of stress which may not be easily achievable via experiment.

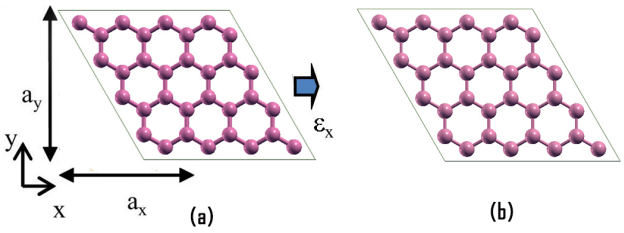

FIGURE 2: Top View Of (a) Pure Silicene And (b) 1% Strained Silicene

The figure Figure 2a illustrates the structure of pure silicene when no strain is applied while figure Figure 2b depicts uniaxial deformation of silicene stretched along the x-direction. For all of the structures, we observed that the periodic sheet size along the transverse direction reduces due to the increment of strain along the x-direction.

TABLE I: Optimized Structural Parameters Of Strained Silicene

Parameters	**0%**	**1%**	**3%**	**5%**	**7%**	**8%**
Lattice parameter (a)	15.48	15.64	15.95	16.26	16.56	16.72
Si-Si lengths (in Å)	2.28	2.30	2.36	2.37	2.42	2.44
Buckling Height (ΔZ in Å)	0.44	0.42	0.36	0.32	0.34	0.33

It is interesting to note that the buckling height of sheets is gradually reduced and the bond lengths/angles between Si atoms are increased on increasing strain. This implies that the buckled structure of pristine Silicene becomes flattered under strain application and finally causes the transformation of hybridization in silicene from sp^3 to sp^2. The results are found to be consistent with the reported data [29]. The deformation or effect of longitudinal strain on the lateral direction can be defined by Poisson's ratio ν.

TABLE II: Deformation Along Lateral Direction Due To Longitudinal Strain Expressed In Terms Of Poisson's Ratio (ν)

Strained Silicene	**1%**	**3%**	**8%**
Poisson's ratio ν	0.08	0.02	0.008

Although values are small (Table Table II), presence of Poisson's ratio indicates the influences on lateral direction due to the strain along the longitudinal direction. Furthermore, decreasing Poisson's ratio with strain implies that the system tends to become less stiffer or more brittle under uniaxial strain.

Formation energy is the useful parameter to analyze the stability of different states of Silicene.

Figure 3 shows that the formation energy increases with the accretion of strain magnitude. This implies that the strained structure is unfavorable under strain. Note that the positive formation energy connotes that the external energy is required to form the structure.

3.2. Electronic Properties

One of the reasons behind immense interest in silicene and graphene is due to the presence of valence and conduction bands with linear dispersion, known as Dirac cones. The Dirac cones exhibit valleys in the Brillouin zone and the two degenerate bands originate from the sublattices of hexagonal structure. In the case of graphene,

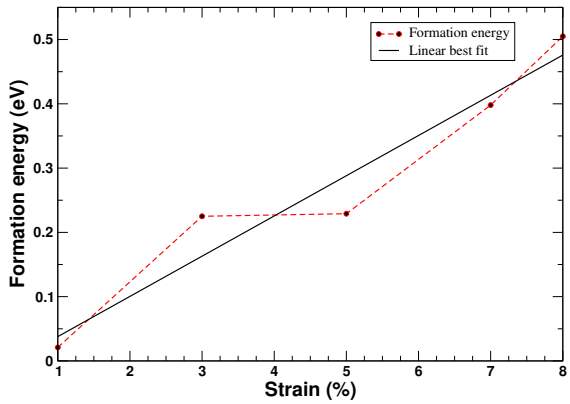

FIGURE 3: Formation Energy Changes With Strain

these Dirac bands stem from the p_z states on each sublattice; and are decoupled from the s and others p_x , p_y states. On the other hand, p_z states are coupled to p_x and p_y states, as well as s states due to lack of mirror symmetry in silicene [16] . Though the presence of Dirac cones was not realized, the first-ever band structure of Silicene was investigated in 1994 [7]. A linear dispersion was argued in 2007.

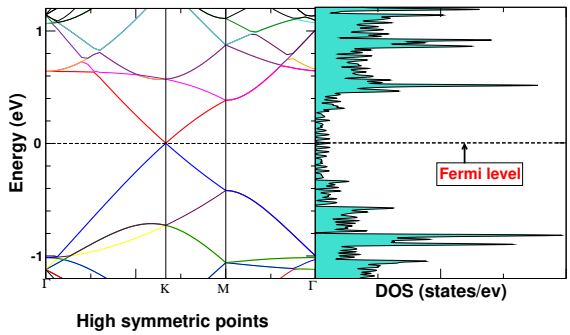

FIGURE 4: Electronic Band Structure And Corresponding DOS Of Pristine Silicene Along With $\Gamma - K - M - \Gamma$ Path Of Brillouin Zone. Energy Levels Have Been Adjusted Relative To Fermi Energy $E_F = -2.858$ eV

Figure 4 proclaims that there is an occurrence of linearly crossing bands, Dirac cones, in Fermi level at K point; this discloses that the charge carriers near Dirac point behave like massless Dirac Fermions. Furthermore, the figure implies the semi-metallic nature of silicene since the value of DOS at E_F is zero, and the conduction and valence band intersect each other only at the high symmetry K point. The contribution of DOS and the energy levels just below and above the Fermi level are predominantly due to π and π^* orbitals.

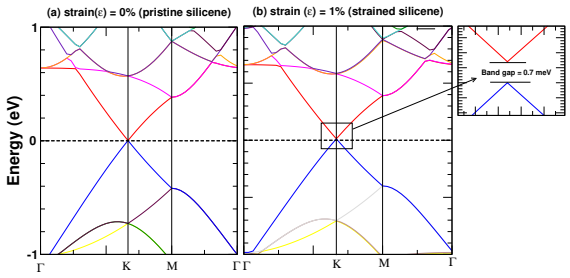

FIGURE 5: Electronic Band Structures Of (a) 4×4 Pristine And (b) 1% Strained Silicene

As we have mentioned that when no strain is applied, the linear energy dispersion relation appears at Dirac (K) point. This illustrates the semiconductor properties with zero band gap; whereas 1% uniaxial strain opens finite but almost negligible band gap of (0.7meV). Further increase in strain causes the energy level at the Γ point shifting up/down and increase in the band gap (Figure 6).

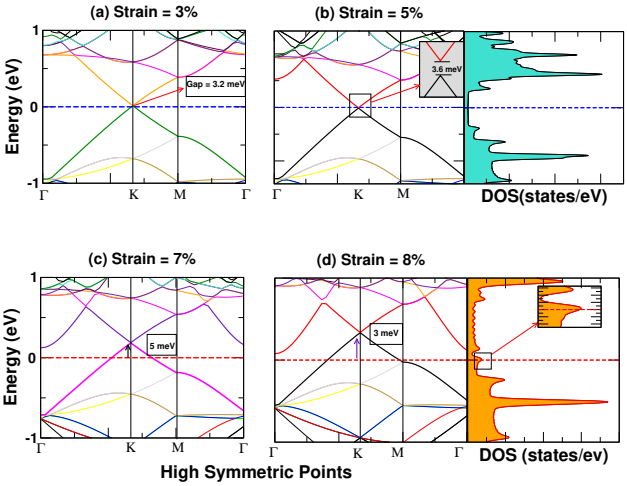

FIGURE 6: Electronic Band Structures And DOS Of (a) 3% Strained, (b) 5 % Strained, (c) 7% Strained, And (d) 8 % Strained Silicene

Figure 6 shows that the Dirac cone persists at the Fermi level for strain up to 5%; however, the Dirac cone shifts above the Fermi level for further increase of strain magnitude. Additionally, the DOS at the Fermi level appears under 7% and 8% strain. In other words, the Fermi level changes its position and exhibits presence of band at the Fermi level (Figure 6 (c) and (d)), which are consistent with the references [17], [18].

TABLE III: Band Gap Induced Under The Influence Of Strain Application

Strain In Systems	Band Gap
1%	0.7 meV
3%	3.2 meV
5%	3.6 meV

Silicene goes into the metallic transition for excessive strain (7% and above). Table Table III shows that the band gap increases up to 5% of the strain and then no gap appears at Fermi level (due to its shifting) at strain of 7% and above. These effects have been observed in energy bands due to breaking of its lattice symmetry. The mismatch in symmetry leads to a shift in the energy levels of conduction and valence bands to change the overall band structure. These results are concord with the reported values [18], [30].

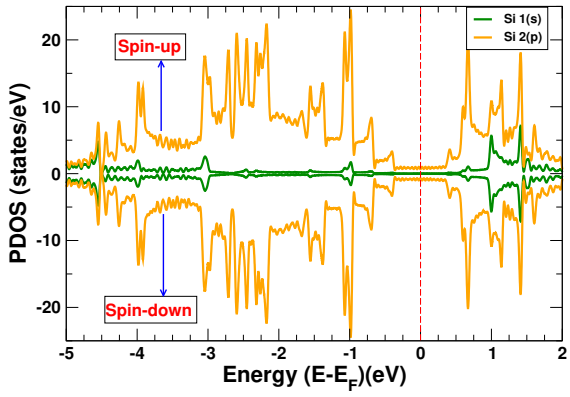

FIGURE 7: PDOS Of Pristine Silicene

Implementing projected density of states (PDOS) calculations, we observed that the valance 2p orbitals of Si contribute the most near the Fermi level for total spin states where as 1s orbitals can also be seen in small peaks. Again, the DOS for s and p orbitals in up and down spin states are exactly symmetrical; this corroborates the non-magnetic nature of silicene.

Analysis of the orbital contributions in strained silicene shows that uniaxial strain shifts their distribution, however, dominance of 2p orbitals nearby the Fermi energy level remain intact.

3.3. Adsorption of Methane

To study the influence of uniaxial strain on reactivity silicene towards non-polar gas like methane, we take three representative strain of silicene: 0%, 3%, and 8%. They also represent zero band gap semiconductor, small gap semiconductor and metallic states respectively.

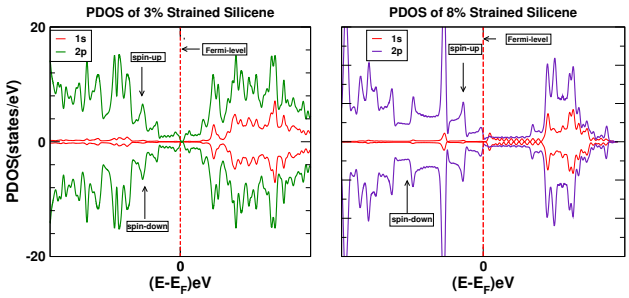

FIGURE 8: PDOS Of Uniaxial 3% And 8% Strained Silicene. The Vertical Dotted Line Represents Fermi-Level Set To Zero

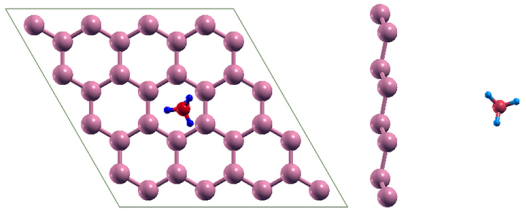

(*) Adsorption of methane (CH_4) on pure silicene

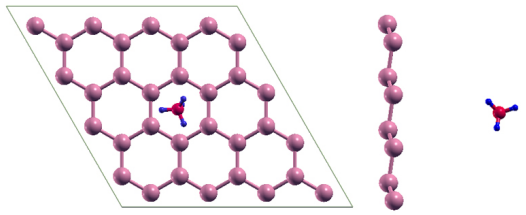

(*) Adsorption on 3% strained silicene

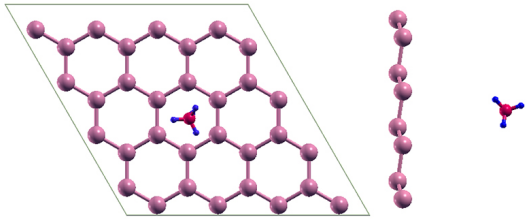

(*) Adsorption on 8% strained silicene

FIGURE 9: Adsorption configurations of methane on silicene at different strain levels

The adsorption energy of CH_4 on strained silicene can be calculated by using equation 3, where the -ve sign favors for adsorption.

Distance in the Table IV represents the shortest distance between carbon atom of methane and the nearest Si atom. Higher the magnitude (negative) of adsorption energy E_{ad} represents the stronger binding of gas

TABLE IV: Adsorption Energy, Band Gap, And Magnetization For Pristine And Strained System Of 4×4 Supercell Silicene After Methane Gas Adsorption

CH_4 Adsorption On	Distance (Å)	Adsorption Energy (eV)	Band Gap	Magnetization
Pristine Si	7.12	-0.17	Dirac-cone	0.00 μ_B/cell
3% strained Si	7.22	-0.42	3.2 meV	0.00 μ_B/cell
8% strained Si	7.30	-0.43	metallic	0.12 μ_B/cell

molecules on the substrate. The table shows that adsorption energy increases on increasing the strain. This is related to stretching of bond lengths and angles with strain which influences the polarity in methane molecule. The tensile/extensive strain causes decrease in overlapping between the orbitals of atoms and weaken the interatomic bonding in host material. This cost of weakening inter-atomic interaction between the atoms of host material improves the host-guest binding, and increases the charge transfer between them [31]. Interestingly, magnitude of adsorption energy meets the standard requirement for the binding of methane at operating condition [20]. The range of adsorption energy (E_{ad} 0.2 eV/molecule to 0.5 eV/molecule) is supposed to be in boarder line of physisorption and weak chemisorption, relevant to vehicular storage [32], and reversible uptake of energy carrying gases [21].

Bader charge analysis calculates the exchange of electronic charge between adsorbent and adsorbate. The higher charge transfer from one of constituents to another implies the stronger interaction between them. Our calculation shows enhancement of charge transfer from silicene to methane on the application of strain. The magnitude starts from 0.0013e for pristine silicene and reaches to 0.015e for 3% strained Silicene into methane molecule. Here the changing pattern of charge transfer is consistent with the adsorption energies: both the parameters (charge transfer and adsorption energy) are higher for strained systems. In all the cases, attraction seems to be dominant by van der Waal's interaction, as similar to the analysis of previous study on silicene Nanoribbons [5].

The band structure and density of states (DOS) calculations after the adsorption of methane gas do not show significant changes with respect to that in without adsorption. This implies that there is no chemical interaction between the constituents, methane and strained silicene. Density functional theory calculations can predict the properties of nanoparticles including two dimensional systems like silicene in atomistic/electronic level, however, can not incorporate the effect of temperature. Also the proper selection of exchange correlation functional may offer challenges in standard DFT calculations.

4. CONCLUSIONS

The influence of uniaxial strain on monolayer (buckled)silicene has been studied to analyze its changes in structural, electronic, and magnetic properties. The strain was increased from 0 to 8%. Pristine (unstrained) silicene forms Dirac cone at the Fermi level where as the band gap appears to be non-zero on increasing strain. However, further increase in strain (at 7% and above) causes shifting of Dirac cone above the Fermi level. Hence the material transits to metallic system.

Furthermore, adsorption behavior of non-polar molecular methane on three different strain-level of silicene: 0% strained, 3% strained, and 8% strained show that methane (CH_4) is physisorbed on all systems. The adsorption energy, however, increases from 0.17 eV (on pristine) to 0.43 eV on the application of uniaxial strain.

Because of buckled structure, its tunability and inherent properties of silicon, it has huge applications in semiconductors, gaseous sensors and storage devices. However, the question of its independent stability is the major issue for its practical application. The increase in gaseous concentration in large surface of silicene may lead to high values of its volumetric and gravitational storage which could be one of the reasons for further study in silicene.

ACKNOWLEDGEMENT

The authors acknowledge computing facility of the Tribhuvan University Research Coordination and Development Council (RCDC) for National Priority Grants TU-NPAR-077/78-ERG-14 and the Supercomputer Centre at the Kathmandu University, Dhulikhel, Nepal which was established with the equipment donated by CERN.

CONFLICT OF INTEREST

The authors declare that there is no conflict of interest.

REFERENCES

1. K. S. Novoselov, A. K. Geim, S. V. Morozov, D. Jiang, Y. Zhang, S. V. Dubonos, I. V. Grigorieva, and A. A. Firsov, science **306**, 666 (2004).
2. M. Dewapriya, R. Rajapakse, and S. Meguid, in *Synthesis, Modeling, and Characterization of 2D Materials, and Their Heterostructures* (Elsevier, 2020) pp. 9–35.
3. J. Zhuang, X. Xu, H. Feng, Z. Li, X. Wang, and Y. Du, Science Bulletin **60**, 1551 (2015).
4. D. Jose and A. Datta, Accounts of chemical research **47**, 593 (2014).
5. S. Aghaei, M. Monshi, and I. Calizo, RSC advances **6**, 94417 (2016).

6. J. Feng, Y. Liu, H. Wang, J. Zhao, Q. Cai, and X. Z. Wang, Computational Materials Science **87**, 218 (2014).
7. K. Takeda and K. Shiraishi, Physical Review B **50**, 14916 (1994).
8. C. Leandri, G. Le Lay, B. Aufray, C. Girardeaux, J. Avila, M. Davila, M. Asensio, C. Ottaviani, and A. Cricenti, Surface science **574**, L9 (2005).
9. G. G. Guzmá Verri and L. L. Y. Voon, Physical Review B **76**, 075131 (2007).
10. B. Feng, Z. Ding, S. Meng, Y. Yao, X. He, P. Cheng, L. Chen, and K. Wu, Nano letters **12**, 3507 (2012).
11. P. De Padova, C. Quaresima, P. Perfetti, B. Olivieri, C. Leandri, B. Aufray, S. Vizzini, and G. Le Lay, Nano letters **8**, 271 (2008).
12. P. Vogt, P. De Padova, C. Quaresima, J. Avila, E. Frantzeskakis, M. C. Asensio, A. Resta, B. Ealet, and G. Le Lay, Physical review letters **108**, 155501 (2012).
13. M. Ieong, B. Doris, J. Kedzierski, K. Rim, and M. Yang, Science **306**, 2057 (2004).
14. L. Sun, Q. Li, H. Ren, H. Su, Q. Shi, and J. Yang, The Journal of chemical physics **129**, 074704 (2008).
15. M. Topsakal and S. Ciraci, Physical Review B **81**, 024107 (2010).
16. L. Y. V. LC, Chinese Physics B **24**, 087309 (2015).
17. R. Qin, C. H. Wang, W. Zhu, and Y. Zhang, Aip Advances **2**, 022159 (2012).
18. S. A. Wella, I. D. Aditya, T. D. K. Wungu, *et al.*, in *Key Engineering Materials*, Vol. 675 (Trans Tech Publ, 2016) pp. 15–18.
19. T. Adhikari, N. Pantha, and N. Adhikari, Journal of Nepal Physical Society **8**, 7 (2022).
20. S. K. Bhatia and A. L. Myers, Langmuir **22**, 1688 (2006).
21. N. Pantha, K. Ulman, and S. Narasimhan, The Journal of Chemical Physics **153**, 244701 (2020).
22. P. Giannozzi, S. Baroni, N. Bonini, M. Calandra, R. Car, C. Cavazzoni, D. Ceresoli, G. L. Chiarotti, M. Cococcioni, and I. Dabo *et al.*, J. Phys. Condens. Matter **21**, 395502 (2009).
23. P. Giannozzi, O. Andreussi, T. Brumme, O. Bunau, M. B. Nardelli, M. Calandra, R. Car, C. Cavazzoni, D. Ceresoli, and M. Cococcioni *et al.*, J. Phys. Condens. Matter **29**, 465901 (2017).
24. P. Giannozzi, O. Baseggio, P. Bonfà, D. Brunato, R. Car, I. Carnimeo, C. Cavazzoni, S. de Gironcoli, P. Delugas, and F. Ferrari Ruffino *et al.*, J. Chem. Phys. **152**, 154105 (2020).
25. J. P. Perdew, K. Burke, and M. Ernzerhof, Phys. Rev. Lett. **77**, 3865 (1996).
26. B. G. Pfrommer, M. Côté, S. G. Louie, and M. L. Cohen, J. Comp. Phys. **131**, 233 (1997).
27. N. Marzari, D. Vanderbilt, A. De Vita, and M. C. Payne, Phys. Rev. Lett. **82**, 3296 (1999).
28. U. Khan, M. U. Saeed, H. O. Elansary, I. M. Moussa, A.-U.-R. Bacha, and Y. Saeed, RSC Advances **14**, 4844 (2024).
29. Q. Peng, X. Wen, and S. De, Rsc Advances **3**, 13772 (2013).
30. H. Zhao, Physics Letters A **376**, 3546 (2012).
31. E. M. Dietze and H. Grönbeck, ChemPhysChem **21**, 2407 (2020).
32. B. C. Wood, S. Y. Bhide, D. Dutta, V. S. Kandagal, A. D. Pathak, S. N. Punnathanam, K. Ayappa, and S. Narasimhan, The Journal of chemical physics **137**, 054702 (2012).